Mutual Coupling Reduction of a Closely Spaced Four-Element MIMO Antenna System Using Discrete Mushrooms

Guohua Zhai, *Member, IEEE*, Zhi Ning Chen, *Fellow, IEEE*, and Xianming Qing, *Senior Member, IEEE*

***Abstract*— A methodology of using five discrete mushroom-like loadings to reduce the mutual coupling of a closely spaced four-element multiple-input multiple-output antenna system is presented in this paper. The occurrence of the loadings concentrates part of the near fields of the substrate integrated cavity-backed slot (SICBS) antenna element and changes the near-field distribution between each antenna elements, so that the mutual coupling between the antenna elements can be greatly reduced. The loaded four-element SICBS antenna system with an overall size of $1.2\lambda_0 \times 1.2\lambda_0 \times 0.11\lambda_0$ (λ_0 is the free-space wavelength at the 2.4 GHz) realizes the mutual coupling reduction of 14 dB between the antenna elements along the diagonal lines with identical polarization, while keeping the mutual coupling of the orthogonally placed adjacent elements unchanged over the band of 2.4–2.485 GHz. With the mutual coupling lower than −35 dB between each antenna element pair, the envelope correlation coefficient is less than 0.005 across the operating bandwidth of 2.4–2.485 GHz.**

***Index Terms*— Multiple input multiple output (MIMO), mushroom loadings, mutual coupling, substrate integrated waveguide (SIW), wireless local area network (WLAN).**

I. Introduction

THE multiple-input multiple-output (MIMO) technology can combat the fading and shadowing problems of the modern wireless communication system within rich multipath environment [1]. Lower envelope correlation coefficient (ECC) is beneficial to better diversity performance of the MIMO system [2]. The mutual coupling and reflection coefficient of the antenna system shows direct influence on the ECC. In addition, the channel capacity and the data transfer rate can be greatly increased with the acceleration of the antenna number adopted in the MIMO system [3]. As examples, 4×4 and 8×8 MIMO techniques have been integrated into the IEEE 802.11n [4] and IEEE 802.11ac [5] standards, respectively. However, within limited size, the closely positioned multiple antenna elements lead to a higher mutual coupling, which degrades the performance of the MIMO system in terms of diversity, channel capacity, efficiency of transmission, sensitivity of receiver, and so on [6]. Therefore, it is a challenge to suppress the mutual coupling between the closely placed antenna elements for a compact MIMO system.

Various technologies have been developed to suppress the mutual coupling between two antenna elements, which can be summarized as the usage of current canceling branches [7], applying defected ground structures [8] and metamaterials [9], as well as the adoption of decoupling matching networks [10]–[12]. Recently, the mutual coupling suppression issue of four-element MIMO antenna system has attracted more and more attention. Four-element dummy array is introduced to decouple four-element MIMO antenna system [13]. The metamaterial-split ring resonators are applied to suppress the mutual coupling of the four-element MIMO antenna system [14], [15]. The planar electromagnetic bandgap (EBG)-mushroom structure has also been adopted to enhance the isolation of the four-element antenna system, which is mainly utilized to reduce the surface-wave coupling according to the bandgap EBG characteristics [16]. However, such a technology is not suitable to achieve ultra-low mutual coupling in a multielement MIMO antenna system when the radiated-field coupling is dominant. In [17], a mushroom wall is proposed to block and absorb the space field/near field from the antenna elements and thus enhances the interelement isolation of the four-element substrate integrated cavity-backed slot (SICBS) antenna system, but the cost is increased due to the adoption of the double-layer substrate, and the realized gain is decreased because of the absorption of part of near fields.

One discrete mushroom-like loading is proposed to suppress the mutual coupling between two closely spaced SICBS antennas recently [18]. To expand this technology, five discrete mushroom-like loadings are proposed to reduce the interelement mutual coupling of the closely spaced four-element MIMO antenna system with the edge-to-edge distance of 5 mm ($0.04\lambda_0$) to achieve ultra-low mutual coupling

Manuscript received January 17, 2016; revised June 22, 2016; accepted August 20, 2016. Date of publication September 19, 2016; date of current version October 4, 2016. This work was supported in part by the Agency for Science, Technology, and Research (A*STAR), Singapore, Metamaterials Program under Grant 0921540097, in part by the Economic Development Board (EDB), Singapore, under the office for space technology and industry (OSTIn) space industry alignment grant ("SIAG") S14-1139-IAF OSTIn-SIAG and S14-1138-IAF OSTIn-SIAG, in part by the Natural Science Foundation of Shanghai under Grant 16ZR1445800, and in part by the Open foundation of the State Key Lab. of Millimeter Waves under Grant 201621. An earlier version of this paper was presented at the 2015 Asia–Pacific Microwave Conference, Nanjing, China, Dec. 6–9, 2015.

G. Zhai is with the Information and Science Technology Department, East China Normal University, Shanghai 200241, China, and also with the Institute for Infocomm Research, Agency for Science, Technology and Research, Singapore 138632 (e-mail: ghzhai@ee.ecnu.edu.cn).

Z. N. Chen is with the Department of Electrical Engineering, National University of Singapore, Singapore 117583 (e-mail: eleczn@nus.edu.sg).

X. Qing is with the Institute for Infocomm Research, Agency for Science, Technology and Research, Singapore 138632 (e-mail: qingxm@i2r.a-star.edu.sg).

Color versions of one or more of the figures in this paper are available online at http://ieeexplore.ieee.org.

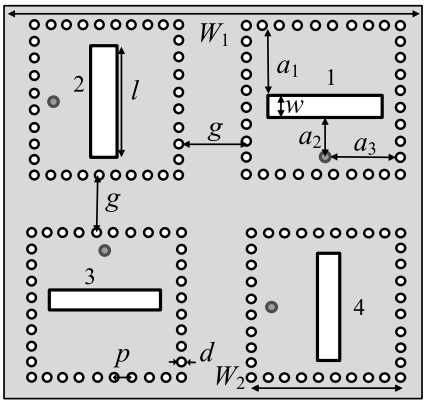

Fig. 1. Geometry of the four-element SICBS antennas. $W_1 = 150$ mm, $a_1 = 22.25$ mm, $a_2 = 17.03$ mm, $a_3 = 24.73$ mm, $W_2 = 49.46$ mm, $l = 48.3$ mm, $w = 4.5$ mm, $d = 0.5$ mm, $p = 0.76$ mm, and $h_1 = 1.524$ mm.

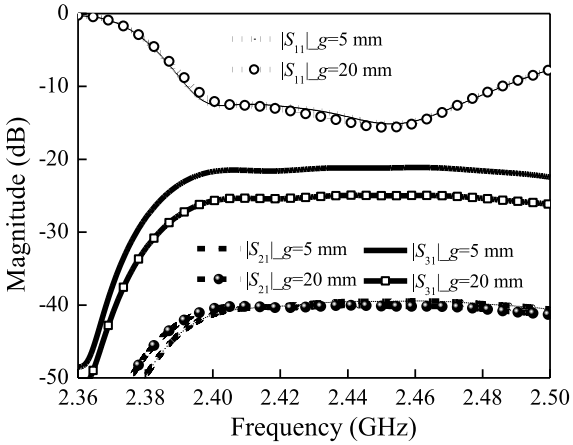

Fig. 2. Mutual coupling of the four-element SICBS antennas with the variation of g.

(lower than -35 dB). The loadings introduce additional nodes and change the near-field distribution between the antenna elements, so that the mutual coupling between the diagonally positioned elements with the same polarization is greatly reduced, while the mutual coupling between the orthogonally placed adjacent elements is kept unchanged.

This paper is organized as follows. In Section II, the interelement coupling of the four-element SICBS antenna system is discussed. Section III presents the methodology of the mushroom-like loadings and the study of its effect on the interelement mutual coupling of the four-element antenna system. Section IV shows the simulated and measured results. A conclusion is presented in Section V. The antenna system is designed and optimized using CST Microwave Studio 15.0.

II. Four-Element SICBS MIMO Antenna System

As discussed in [19], an orthogonal positioned MIMO antenna system is able to achieve ultra-low mutual coupling between the antenna elements along the diagonal line and then offers higher capacity and more flexibility for the system. The SICBS antenna elements with the same edge-to-edge distance (g) between the adjacent elements are orthogonally distributed, as shown in Fig. 1. Consider the antenna system as a reciprocal and symmetrical four-port network, $Z_{12} = Z_{14} = Z_{23} = Z_{34} = Z_{21} = Z_{32} = Z_{43} = Z_{41}$, $Z_{11} = Z_{22} = Z_{33} = Z_{44}$, $Z_{13} = Z_{24} = Z_{31} = Z_{42}$. The impedance matrix is written as

$$\boldsymbol{Z} = \begin{bmatrix} Z_{11} & Z_{12} & Z_{13} & Z_{12} \\ Z_{12} & Z_{11} & Z_{12} & Z_{13} \\ Z_{13} & Z_{12} & Z_{11} & Z_{12} \\ Z_{12} & Z_{13} & Z_{12} & Z_{11} \end{bmatrix} \tag{1}$$

where $\boldsymbol{Z}$ can be calculated according to the S-parameters of the four-element MIMO antenna system as

$$\boldsymbol{Z} = (\boldsymbol{I} + \boldsymbol{S})^{-1})(\boldsymbol{I} - \boldsymbol{S}) \tag{2}$$

where $\boldsymbol{I}$ is the unit matrix and $\boldsymbol{S}$ is the scatter matrix of the four-element MIMO antenna system. Similar to $\boldsymbol{Z}$ matrix, the $\boldsymbol{S}$-matrix can be written as

$$\boldsymbol{S} = \begin{bmatrix} S_{11} & S_{12} & S_{13} & S_{12} \\ S_{12} & S_{11} & S_{12} & S_{13} \\ S_{13} & S_{12} & S_{11} & S_{12} \\ S_{12} & S_{13} & S_{12} & S_{11} \end{bmatrix} \tag{3}$$

where S_{12} is the mutual coupling between the adjacent elements and S_{13} is the mutual coupling between the diagonal ones. Clearly, the lower the mutual coupling becomes, the smaller the mutual impedance is achieved.

The four-element SICBS antenna system is designed on a single-layer Rogers 5880 with a thickness of $h_1 = 2.5$ mm, ε_r of 2.2, and tanδ of 0.0009. For brevity, only $|S_{11}|$, $|S_{21}|$, and $|S_{31}|$ are presented in the following discussion. The parameter of g of 5 mm ($0.04\lambda_0$) and 20 mm ($0.16\lambda_0$) is selected as an example for smaller and larger separation, respectively. Its effect on the S-parameters of the four-element antenna system is shown in Fig. 2. It is found that the changing of g has slight effect on the reflection coefficient over the 2.4-GHz wireless local area network (WLAN) band of 2.4–2.485 GHz.

When $g = 5$ mm, it is observed that the orthogonally positioned antenna pairs achieve the lower interelement mutual coupling of $|S_{21}| < -40$ dB while the parallel positioned element pairs exhibit the larger one of $|S_{31}| < -21$ dB within the operating bandwidth. Meanwhile, $|S_{31}|$ is decreased by about 3 dB, while $|S_{21}|$ remains unchanged as g increases from 5 to 20 mm.

III. Decoupling Technique With Dummy Loadings

A. Decoupling Technique Using Discrete Mushroom Loadings

In this paper, five discrete mushroom-like loadings are proposed to reduce the mutual coupling of the four-element MIMO antenna system as shown in Fig. 3, wherein each loading comprises two metallic discs and a grounded post. The post connects the discs and extends to the ground plane. Five loadings are positioned in between the antenna elements wherein one is positioned in the center and the other four are

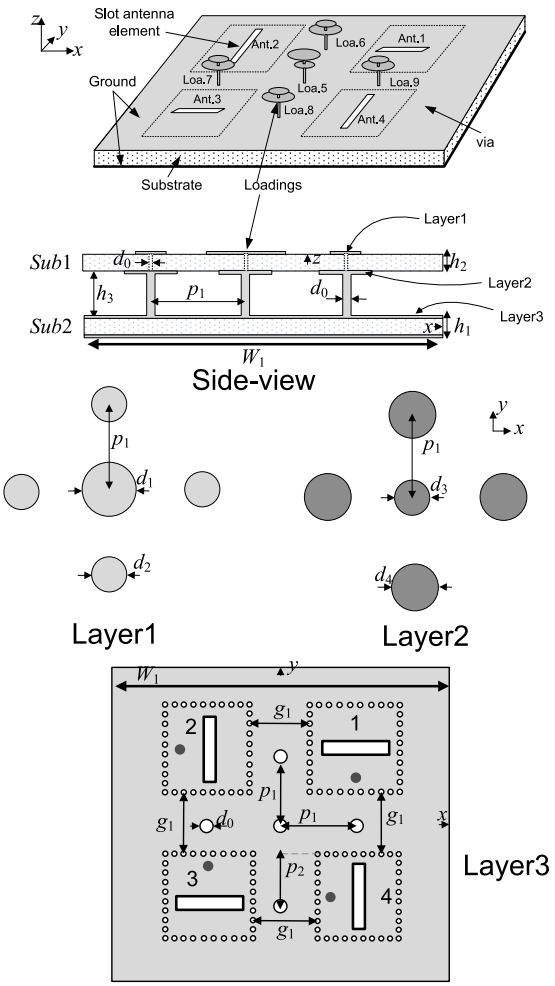

Fig. 3. Geometry of the four-element SICBS antenna system with mushroom loadings.

placed at the left/right and upper/lower sides symmetrically. The four-element SICBS elements are symmetrically arranged at the identical edge-to-edge distance of g, and separately fed by the coaxial probes, respectively. Note that the labels Ant. n ($n = 1, 2, 3, 4$) and Loa. m ($m = 0, 1, 2, 3, 4$) indicate the antenna elements and the dummy loadings, respectively.

The circular metallic patches of the loadings are etched on the opposite sides of the top substrate with a thickness of h_2. The grounded posts are with the same radius of d_0 and height of h_3. The radii of the patches of the center mushroom cell are d_1 and d_3, respectively. The radii of the patches of the surrounding loadings are d_2 and d_4, respectively. Furthermore, the surrounding loadings are with the same separation of p_1 from the center one. The four SICBS antenna elements are implemented on the lower substrate with a thickness of h_1.

The planar EBG-mushroom structure has been widely applied to suppress the mutual coupling of the multielement antenna system, which is mainly utilized to reduce the surface-wave coupling according to the bandgap EBG characteristics [16]. However, such a technology is not suitable to achieve ultra-low mutual coupling in multielement MIMO antenna system when the radiated-field coupling is dominant. In this paper, the proposed discrete mushroom loadings with the height around $0.1\lambda_0$ will change the near-field distribution and influence the inter-between mutual impedance of the MIMO antenna system. Meanwhile, only five mushroom cells are positioned in between the antenna elements wherein one is positioned in the center and the other four are placed sequentially inter-between adjacent elements.

B. Network Analysis

Considering the four-element MIMO SICBS antenna system and the five-element discrete loadings as a night-element antenna system, its impedance matrix can be written as

$$\boldsymbol{Z} = \begin{bmatrix} \boldsymbol{Z_{AA}} & \boldsymbol{Z_{AL}} \\ \boldsymbol{Z_{LA}} & \boldsymbol{Z_{LL}} \end{bmatrix} \tag{4}$$

where $\boldsymbol{Z_{AA}}$ and $\boldsymbol{Z_{LL}}$ are the impedance matrices of the four antenna element and five dummy loading elements, $\boldsymbol{Z_{AL}}$ and $\boldsymbol{Z_{LA}}$ are the mutual impedance matrices between the antenna elements and dummy loading elements, respectively. $\boldsymbol{Z_{AA}}$ is written as (1), and $\boldsymbol{Z_{LL}}$ is written as

$$\boldsymbol{Z_{LL}} = \begin{bmatrix} Z_{55} & Z_{56} & Z_{57} & Z_{58} & Z_{59} \\ Z_{65} & Z_{66} & Z_{67} & Z_{68} & Z_{69} \\ Z_{75} & Z_{76} & Z_{77} & Z_{78} & Z_{79} \\ Z_{85} & Z_{86} & Z_{87} & Z_{88} & Z_{89} \\ Z_{95} & Z_{96} & Z_{97} & Z_{98} & Z_{99} \end{bmatrix} \tag{5}$$

where Z_{ij} is the mutual impedance between Loa. i and Loa. j, and Z_{ii} is the self-impedance of the Loa. i. The surrounding loadings of Loas. 6–9 are identical owing to the symmetrical and reciprocal structure, so $Z_{56} = Z_{57} = Z_{58} = Z_{59} = Z_{65} = Z_{75} = Z_{85} = Z_{95}$, $Z_{67} = Z_{78} = Z_{89} = Z_{96} = Z_{69} = Z_{98} = Z_{87} = Z_{76}$, $Z_{66} = Z_{77} = Z_{88} = Z_{99}$, $Z_{68} = Z_{79} = Z_{86} = Z_{97}$. The matrix of $\boldsymbol{Z_{LL}}$ can be simplified as

$$\boldsymbol{Z_{LL}} = \begin{bmatrix} Z_{55} & Z_{56} & Z_{56} & Z_{56} & Z_{56} \\ Z_{56} & Z_{66} & Z_{67} & Z_{68} & Z_{67} \\ Z_{56} & Z_{67} & Z_{66} & Z_{67} & Z_{68} \\ Z_{56} & Z_{68} & Z_{67} & Z_{66} & Z_{67} \\ Z_{56} & Z_{67} & Z_{68} & Z_{67} & Z_{66} \end{bmatrix}. \tag{6}$$

$\boldsymbol{Z_{AL}}$ is written as

$$\boldsymbol{Z_{AL}} = \begin{bmatrix} Z_{15} & Z_{16} & Z_{17} & Z_{18} & Z_{19} \\ Z_{25} & Z_{26} & Z_{27} & Z_{28} & Z_{29} \\ Z_{35} & Z_{36} & Z_{37} & Z_{38} & Z_{39} \\ Z_{45} & Z_{46} & Z_{47} & Z_{48} & Z_{49} \end{bmatrix} \tag{7}$$

where Z_{ij} is the mutual impedance between Ant. i and Loa. j. Similar to the matrices of $\boldsymbol{Z_{AA}}$ and $\boldsymbol{Z_{LL}}$, $\boldsymbol{Z_{AL}}$ can be further simplified according to the symmetrical characteristics of the four-element antenna system with the dummy loadings. It is rewritten as

$$\boldsymbol{Z_{AL}} = \begin{bmatrix} Z_{15} & Z_{16} & Z_{17} & Z_{18} & Z_{19} \\ Z_{15} & Z_{19} & Z_{16} & Z_{17} & Z_{18} \\ Z_{15} & Z_{18} & Z_{19} & Z_{16} & Z_{17} \\ Z_{15} & Z_{17} & Z_{18} & Z_{19} & Z_{16} \end{bmatrix}. \tag{8}$$

The matrix of $\boldsymbol{Z_{LA}}$ is a transpose of $\boldsymbol{Z_{AL}}$, which means that $\boldsymbol{Z_{LA}} = \boldsymbol{Z_{AL}}^{\mathrm{T}}$ as shown

$$\boldsymbol{Z_{LA}} = \begin{bmatrix} Z_{15} & Z_{15} & Z_{15} & Z_{15} \\ Z_{16} & Z_{19} & Z_{18} & Z_{17} \\ Z_{17} & Z_{16} & Z_{19} & Z_{18} \\ Z_{18} & Z_{17} & Z_{16} & Z_{19} \\ Z_{19} & Z_{18} & Z_{17} & Z_{16} \end{bmatrix}. \tag{9}$$

Each mushroom cell can be considered as an open ended transmission line loaded with a capacitor, the impedances of the surrounding four loadings (Loas. 6–9) and the center one (Loa. 5) as Z_{L1} and Z_{L2}, which can be defined as

$$Z_{L1} = Z_0 \frac{Z_{c1} + jZ_0 \tan \beta l}{Z_0 + jZ_{c1} \tan \beta l} \tag{10}$$

$$Z_{L2} = Z_0 \frac{Z_{c2} + jZ_0 \tan \beta l}{Z_0 + jZ_{c2} \tan \beta l} \tag{11}$$

where Z_0, β, and l are the characteristic impedance, phase constant, and length of the transmission line, respectively. Z_{c1} and Z_{c2} are the equivalent impedance of the top double-layer patches for Loas. 6–9 and Loa. 5, respectively. The details of Z_{c1} and Z_{c2} calculation can be found in [20].

Considering the ports of the five discrete mushroom loadings as passive, then its impedance matrix is written as

$$\boldsymbol{Z'_{LL}} = \begin{bmatrix} Z_{L2} & 0 & 0 & 0 & 0 \\ 0 & Z_{L1} & 0 & 0 & 0 \\ 0 & 0 & Z_{L1} & 0 & 0 \\ 0 & 0 & 0 & Z_{L1} & 0 \\ 0 & 0 & 0 & 0 & Z_{L1} \end{bmatrix}. \tag{12}$$

The impedance matrix of the four-element SICBS MIMO antenna system loaded with five-discrete mushroom-like loadings is written as

$$\boldsymbol{Z'_{AA}} = \begin{bmatrix} Z'_{11} & Z'_{12} & Z'_{13} & Z'_{12} \\ Z'_{12} & Z'_{11} & Z'_{12} & Z'_{13} \\ Z'_{13} & Z'_{12} & Z'_{11} & Z'_{12} \\ Z'_{12} & Z'_{13} & Z'_{12} & Z'_{11} \end{bmatrix}. \tag{13}$$

According to the microwave network analysis in [13] and [21], it can be calculated as

$$\boldsymbol{Z'_{AA}} = \boldsymbol{Z_{AA}} + \boldsymbol{Z_{AL}}(\boldsymbol{Z'_{LL}} - \boldsymbol{Z_{LL}})^{-1}\boldsymbol{Z_{LA}}. \tag{14}$$

It is clear that the mutual impedance between the four-element MIMO SICBS antenna system is determined by the parameters of Z_{L1} and Z_{L2}, which is related with the type, distance, and height of the loadings. The network analysis helps the understanding of the effect of the loading structures on the mutual coupling between the antenna elements. The initial value of the key parameters of the loadings, such as h_3, p_1, and d_0–d_4, can be primarily set according to the near-field distribution of the system with mushroom as discussed in the following.

C. Fields Distribution

When Ant. 1 is excited at 2.44 GHz, the E-field distribution in xy and xz planes is shown in Fig. 4. Owing to the introduction of the mushroom cells, the majority of field is concentrated between Ant. 1 and Loa. 9, and thus, very little

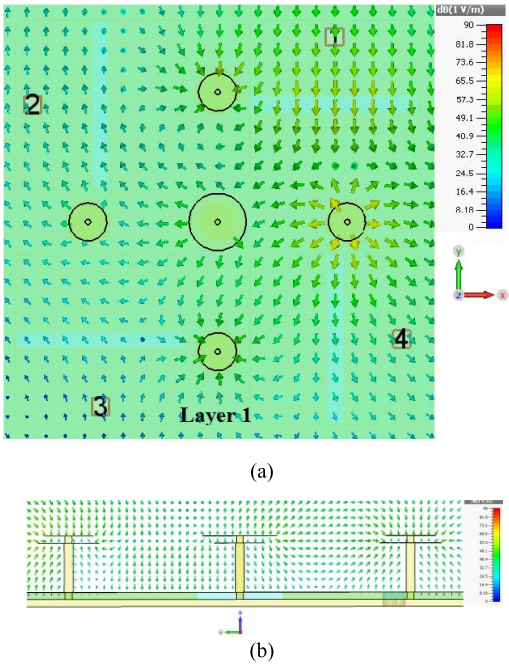

Fig. 4. Simulated E-field distribution at 2.44 GHz. (a) Layer 1 (xy plane, $z = 13.67$ mm). (b) Cross-sectional view (xz plane, $y = 0$ mm) (excited by Ant. 1).

field is coupled to other antenna elements. Meanwhile, the orientation of the electric field around Ant. 3 is changed. First, the direction of the electric field is no more completely parallel to that of Ant. 1. There is an oblique angle between the E-field and the slot of the Ant. 3. Second, the field distributed along the two ends of the Ant. 3 is opposite because of the two adjacent electric nodes induced by Loa. 7 and Loa. 8, respectively. In addition, the electric field around Ant. 2 and Ant. 4 shows little change compared with that without mushroom cells because of the major orthogonal role between the adjacent antenna pair. Therefore, the mushroom loading disturbs the distribution of the near field and leads to a change of the field orientation. Thus, the mutual coupling between the antenna elements along the diagonal lines is greatly suppressed.

As shown in Fig. 4(b), there are a few electric fields between the upper disc and the lower one of a mushroom cell, which provides a small capacitance. While there are a lot of fields distributed between the center one with adjacent one, which provide a large capacitance. The long conducting path along posts links them together to form a loop, which provides the inductance. Therefore, the operating frequency of the mushroom loading can be evaluated as

$$2h_3 + p_1 = \lambda_0/2 \tag{15}$$

$$\pi d_4 + 2h_3 = \lambda_0/2 \tag{16}$$

$$p_1 = p_2 + g/2 \approx (W_2 + g)/2. \tag{17}$$

Fig. 5 compares the E-fields magnitude distribution of the antenna system with/without mushroom loading. The 3-D E-field distribution at 2.44 GHz is shown in Fig. 6. Because Loa. 9 is positioned at one side of Ant. 1, induced field is tightly concentrated around Loa. 9. It can be considered as the extension of the field radiated from Ant. 1, and thus serves as another half-wavelength radiator, which can

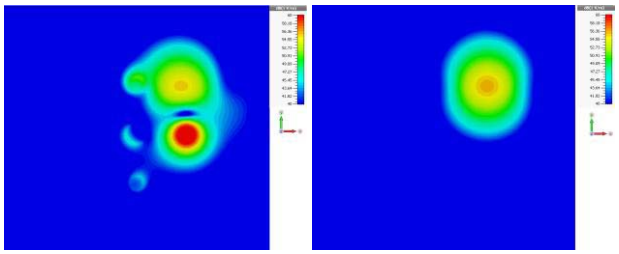

(a) (b)

Fig. 5. Simulated E-filed magnitude distribution along the xy plane at 2.44 GHz (excited by Ant. 1, $z = 13.67$ mm). (a) With mushroom. (b) Without mushroom.

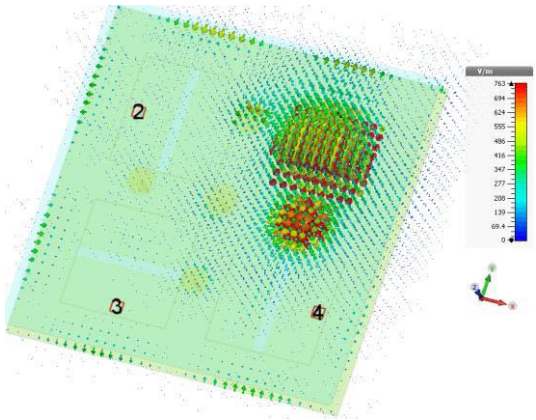

Fig. 6. 3-D E-field distribution of the proposed four-element antenna system with mushroom at 2.44 GHz (excited by Ant. 1).

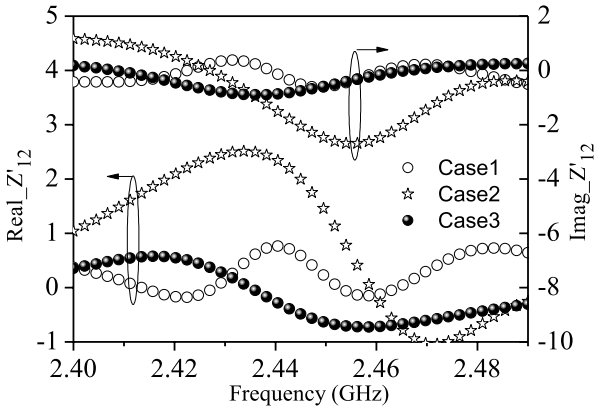

(a)

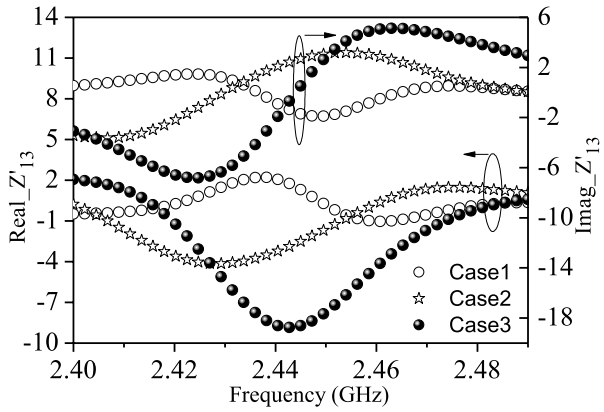

(b)

Fig. 7. (a) Z'_{12} with different parameters of mushroom loadings. (b) Z'_{13} with different parameters of loadings.

be expressed as (16). In addition, the low Q-factor of the mushroom loading benefits from the large electric distance between mushroom cells and the length of the post, which leads to very small losses induced by the mushroom structure. Therefore, the variation of the antenna efficiency will be trivial.

The relation between the position of the mushroom and the parameter of g is actually included in the description of the parameter of p_1. The distance between the adjacent SICBS antennas can be preset according to (17), where p_2 is close to the half width of the substrate integrated waveguide (SIW) cavity, namely, W_2.

D. Parameter Optimization

For studying the effects of the loadings on Z'_{12} and Z'_{13}, three different cases of the antenna system with the mushroom are defined as follows.

1) *Case 1:* $d_1 = 20$ mm, $d_2 = 2$ mm, $d_3 = 20$ mm, $d_4 = 14$ mm, and $h_3 = 10.5$ mm.
2) *Case 2:* $d_1 = d_2 = d_3 = d_4 = 12$ mm, and $h_3 = 8$ mm.
3) *Case 3:* The antenna system without mushroom.

The other parameters of the antenna system with loadings are constant as: $d_0 = 2$ mm, $w = 3.4$ mm, $p = 0.76$ mm, $a_1 = 21$ mm, $p_1 = 35.32$ mm, $l = 51.4$ mm, $a_2 = 29$ mm, $g = 5$ mm, $W_2 = 60.9$ mm, and $a_3 = 30$ mm. Fig. 7 shows Z'_{12} and Z'_{13} of the three scenarios over the 2.4-GHz WLAN band of 2.4–2.485 GHz. It can be seen that Z'_{12} of Case 2 vary larger than that both of Cases 1 and 3, and Z'_{13} of Case 3 vary larger than that both of Cases 1 and 2. The real and imaginary parts of Z'_{12} and Z'_{13} of Case 1 are around zero, which indicates that the goal of the minimum values both of Z'_{12} and Z'_{13} can be achieved by adjusting the parameters of loadings.

The height of the mushroom cell (h_3) is first preset as about $0.1\lambda_0$, and then, the periodic of the mushroom cell, namely p_1, is estimated according to (15). The radius of the peripheral disc printed in the layer 2 (d_4) is determined by (16). The distance between the adjacent SIW cavities, namely, g, is calculated according to (17). The parameters of d_0–d_3 can be first equal to d_4. Then, the relation between the S-matrix of the four-element SICBS MIMO antenna system with the physical parameters of h_3, p_1, and d_0–d_4 can be built using full wave simulation software, CST, and the relation between the mutual impedance of $\boldsymbol{Z}'_{12}$ and $\boldsymbol{Z}'_{13}$ with the parameters of distribution and geometry of the loadings can be calculated using (2) and (4)–(14). Finally, based on the effect of the parameters of h_3, p_1, and d_0–d_4 on the mutual impedance as discussed earlier, the dimensions of the posts and discs are optimized to achieve the goal of both the real and imagine parts of $\boldsymbol{Z}'_{12}/\boldsymbol{Z}'_{13}$ less than 1. The detailed parameters of the optimized four-element antenna system with mushroom are: $d_0 = 2$ mm, $d_1 = 20$ mm, $d_2 = 8$ mm, $d_3 = 19.4$ mm, $d_4 = 13.68$ mm, $a_1 = 21$ mm, $a_2 = 29$ mm, $a_3 = 30$ mm, $p = 0.76$ mm, $p_1 = 35.32$ mm, $d_1 = 20$ mm, $W_1 = 150$ mm, $W_2 = 60.9$ mm, $h_3 = 10.5$ mm, $w = 3.4$ mm, $l = 51.4$ mm, and $g = 5$ mm.

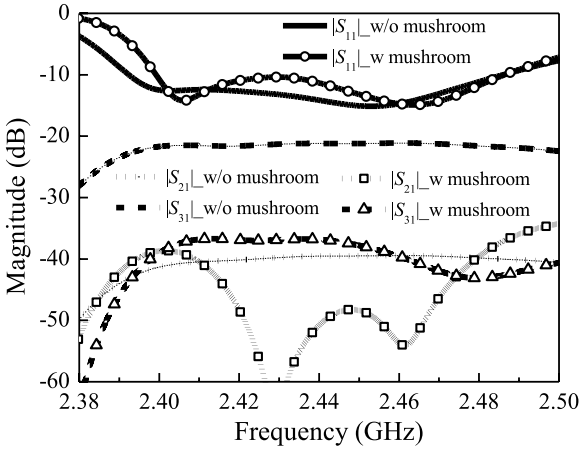

Fig. 8. Comparison of the simulated S-parameters of the four-element antenna system with/without mushroom.

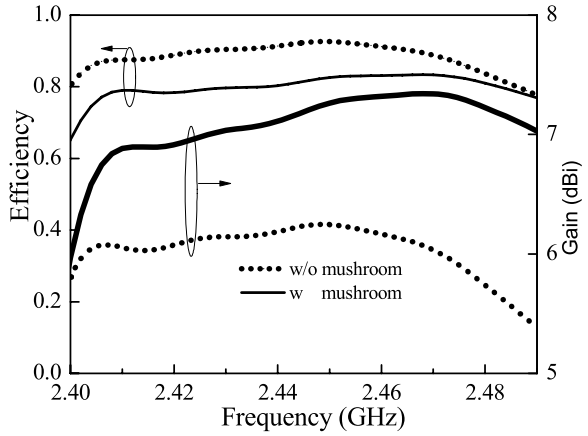

Fig. 9. Comparison of the simulated S-parameters of the four-element antenna system with/without mushroom.

The impedance matching and the interelement coupling of the four-element SICBS antenna system with/without the mushroom structure are compared in Fig. 8. It is observed that without mushroom structure, the $|S_{21}|$ is less than -40.5 dB and $|S_{31}|$ is around -22 dB from 2.4 to 2.485 GHz. With the occurrence of the mushroom structure, the $|S_{21}|$ is less than -37.5 dB, and the $|S_{31}|$ is less than -36.5 dB from 2.4 to 2.485 GHz. Especially, $|S_{21}|$ is less than -42.5 dB from 2.41 to 2.47 GHz. It can be seen that $|S_{31}|$ of the four-element SICBS antenna system can be improved 14.5 dB, while $|S_{21}|$ alters little crossing the band of 2.4–2.485 GHz by loading with a mushroom structure. Therefore, the mutual coupling of the close-spaced four-element SICBS MIMO antenna system can be reduced by 14.5 dB using five discrete mushroom loadings.

The efficiency and the gain of the four-element SICBS antenna system with/without the mushroom structure are compared in Fig. 9. It is observed that the efficiency is just reduced by 0.09 due to the losses of the substrate and ohmic losses of the metallic discs of the mushroom loadings. However, compared with that of the system without mushroom, the realized gain of antenna is increased by 1.4 dB owing to the enlargement of the efficient radiation aperture when the

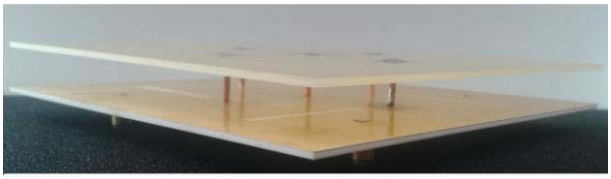

(a)

(b)

Fig. 10. Photograph of the antenna system prototype. (a) Perspective view. (b) Top view.

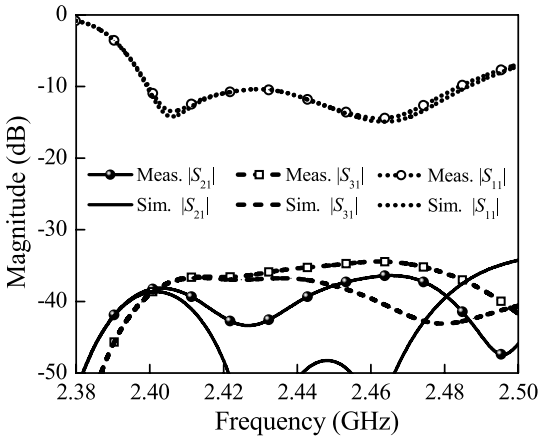

Fig. 11. Measured S-parameters of the four-element SICBS antenna system with mushroom.

near fields are concentrated around the adjacent loading cell positioned to the side of the radiated element.

IV. Fabrication and Measurement

The antenna system with five discrete loadings is fabricated and measured. Two pieces of 1.57-/0.78-mm-thick Rogers 5880 board glued together by a 0.15-mm-thick RO3001 ($\varepsilon_r = 2.28$ and $\tan\delta = 0.003$) prepreg sheet form the 2.5-mm-thick bottom SICBS antenna system. The patches of the mushroom are printed on both sides of a piece of 1.4-mm-thick Fr4 board. The edge-to-edge distance between the adjacent elements is only $0.04\lambda_0$ (5 mm). The antenna prototype shown in Fig. 10 is with an overall size of $1.2\lambda_0 \times 1.2\lambda_0 \times 0.11\lambda_0$ ($150 \times 150 \times 14.4$ mm^3).

The simulated and measured S-parameters of the antenna prototype are shown in Fig. 11. It can be seen that the measured reflection coefficient agrees well with the

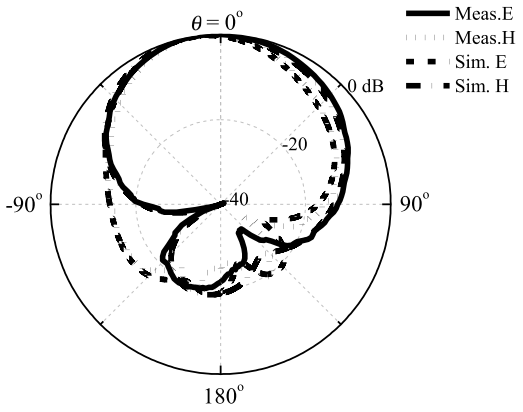

Fig. 12. Measured and simulated radiation patterns (2.44 GHz).

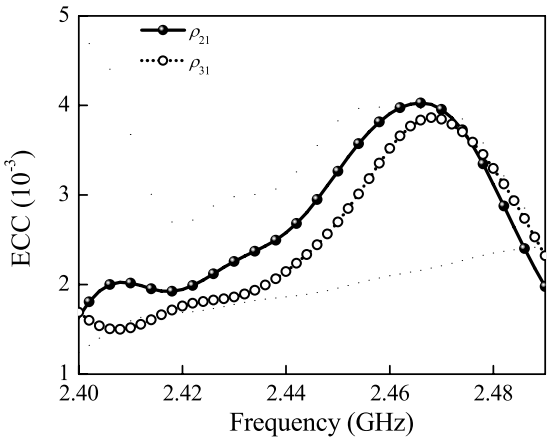

Fig. 13. Calculated ECC of the four-element antenna system.

simulated one. The measured impedance bandwidth for the reflection coefficient of less than −10 dB ranges from 2.4 to 2.485 GHz. The measured $|S_{21}|$ and $|S_{31}|$ show good agreement with the simulations as well. The little difference between the simulated and measured mutual couplings may be attributed to fabrication tolerance and in-house antenna assembly. Note that both of $|S_{21}|$ and $|S_{31}|$ are less than −35 dB in the range from 2.4 to 2.485 GHz. In addition, for the four-element SICBS antenna system with discrete mushroom loadings, the measured maximum realized gain of 7.1 dBi is achieved at 2.46 GHz, which is decreased by 0.5 dB compared with that without wall.

The simulated and measured far-field radiation pattern of Ant. 1 with the mushroom at 2.44 GHz is shown in Fig. 12. Good agreement between the measurement and the simulation can be observed. In both E- and H planes, the front-to-back ratio is larger than 15 dB ranging from 2.4 to 2.485 GHz.

The ECC (ρ_{ij}) shown in Fig. 13 can be calculated using (18) with the simulated 3-D far fields [2] because of good agreement between the simulated and measured patterns

$$\rho_{ij} = \frac{|\iint_{4\pi} [\mathbf{F}_i(\theta,\phi) \cdot \mathbf{F}_j^*(\theta,\phi)] d\Omega|^2}{\iint_{4\pi} |\mathbf{F}_i(\theta,\phi)|^2 d\Omega \iint_{4\pi} |\mathbf{F}_j(\theta,\phi)|^2 d\Omega} \tag{18}$$

where $\mathbf{F}_i(\theta, \varphi)$ is a complex vector indicating the field radiated from the ith element, and symbols $\cdot$ and $*$ denote the Hermitian product and complex conjugate, respectively [2]. Similar to the S-parameters of the antenna system, $\rho_{21} = \rho_{32} = \rho_{43} = \rho_{41}$, and $\rho_{31} = \rho_{42}$. For brevity, only ρ_{21} and ρ_{31} are presented. It can be seen that the ECC is always below 0.005 over the whole impedance bandwidth, indicating the good MIMO performance of the proposed four-element antenna system.

V. Conclusion

The discrete mushroom-like loadings have been proposed to enhance the interelement isolation of a four-element SICBS antenna system for MIMO applications. The field radiated from the antenna elements has been found tightly concentrated between the antenna element and adjacent mushrooms so that ultra-low interelement coupling has been achieved. The measured results have validated the simulation with the interelement coupling of less than −36 dB and ECC lower than 0.005 over the 2.4-GHz WLAN band of 2.4–2.485 GHz.

References

[1] A. J. Paulraj, D. A. Gore, R. U. Nabar, and H. Bolcskei, "An overview of MIMO communications—A key to gigabit wireless," *Proc. IEEE*, vol. 92, no. 2, pp. 198–218, Feb. 2004.

[2] R. G. Vaughan and J. B. Andersen, "Antenna diversity in mobile communications," *IEEE Trans. Veh. Technol.*, vol. VT-36, no. 4, pp. 149–170, Nov. 1987.

[3] J. Thaysen and K. B. Jakobsen, "Envelope correlation in (*N*, *N*) MIMO antenna array from scattering parameters," *Microw. Opt. Technol. Lett.*, vol. 48, no. 5, pp. 832–834, May 2006.

[4] *IEEE Standard for Information Technology-Telecommunications and Information Exchange between Systems-Local and Metropolitan Area Networks-Specific Requirements: Part 11: Wireless LAN Medium Access Control (MAC) and Physical Layer (PHY) Specifications Amendment 5: Enhancements for Very High Throughput*, IEEE Standard 802.11n-2009, Oct. 2009.

[5] *IEEE Standard for Information Technology Telecommunications and Information Exchange Between Systems Local and Metropolitan Area Networks Specific Requirements: Part 11: Wireless LAN Medium Access Control (MAC) and Physical Layer (PHY) Specifications Amendment 4: Enhancements for Very High Throughput for Operation in Bands Below 6 GHz*, IEEE Standard 802.11ac-2013, Dec. 2013.

[6] J. Weber, C. Volmer, K. Blau, R. Stephan, and M. A. Hein, "Miniaturized antenna arrays using decoupling networks with realistic elements," *IEEE Trans. Microw. Theory Techn.*, vol. 54, no. 6, pp. 2733–2740, Jun. 2006.

[7] S. Farsi, H. Aliakbarian, D. Schreurs, B. Nauwelaers, and G. A. E. Vandenbosch, "Mutual coupling reduction between planar antennas by using a simple microstrip U-section," *IEEE Antennas Wireless Propag. Lett.*, vol. 11, pp. 1501–1503, Nov. 2012.

[8] Y. Chung, S.-S. Jeon, D. Ahn, J.-I. Choi, and T. Itoh, "High isolation dual-polarized patch antenna using integrated defected ground structure," *IEEE Microw. Wireless Compon. Lett.*, vol. 14, no. 1, pp. 4–6, Jan. 2004.

[9] L. Yang, M. Fan, F. Chen, J. She, and Z. Feng, "A novel compact electromagnetic-bandgap (EBG) structure and its applications for microwave circuits," *IEEE Trans. Microw. Theory Techn.*, vol. 53, no. 1, pp. 183–190, Jan. 2005.

[10] L. K. Yeung and Y. E. Wang, "Mode-based beamforming arrays for miniaturized platforms," *IEEE Trans. Microw. Theory Techn.*, vol. 57, no. 1, pp. 45–52, Jan. 2009.

[11] L. Zhao, K.-W. Qian, and K.-L. Wu, "A cascaded coupled resonator decoupling network for mitigating interference between two radios in adjacent frequency bands," *IEEE Trans. Microw. Theory Techn.*, vol. 62, no. 11, pp. 2680–2688, Nov. 2014.

[12] K. Qian, L. Zhao, and K.-L. Wu, "An LTCC coupled resonator decoupling network for two antennas," *IEEE Trans. Microw. Theory Techn.*, vol. 63, no. 10, pp. 3199–3207, Oct. 2015.

[13] L. Y. Zhao and K.-L. Wu, "A decoupling technique for four-element symmetric arrays with reactively loaded dummy elements," *IEEE Trans. Antennas Propag.*, vol. 62, no. 8, pp. 4416–4421, Aug. 2014.

[14] D. K. Ntaikos and T. V. Yioultsis, "Compact split-ring resonator-loaded multiple-input–multiple-output antenna with electrically small elements and reduced mutual coupling," *Proc. Inst. Elect. Eng.—Microw., Antennas Propag.*, vol. 7, no. 6, pp. 421–429, Jun. 2013.
[15] A. A. Gheethan, P. A. Herzig, and G. Mumcu, "Compact 2 × 2 coupled double loop GPS antenna array loaded with broadside coupled split ring resonators," *IEEE Trans. Antennas Propag.*, vol. 61, no. 6, pp. 3000–3008, Jun. 2013.
[16] S. Ghosh, T.-N. Tran, and T. Le-Ngoc, "Dual-layer EBG-based miniaturized multi-element antenna for MIMO systems," *IEEE Trans. Antennas Propag.*, vol. 62, no. 8, pp. 3985–3997, Aug. 2014.
[17] G. Zhai, Z. Chen, and X. Qing, "Enhanced isolation of a closely spaced four-element MIMO antenna system using metamaterial mushroom," *IEEE Trans. Antennas Propag.*, vol. 63, no. 8, pp. 3362–3370, Aug. 2015.
[18] G. Zhai, Z. N. Chen, X. Qing, and M. Jiang, "Isolation enhancement between two closely spaced substrate integrated cavity-backed slot antennas using mushroom," in *Proc. IEEE Asia–Pacific Microw. Conf.*, vol. 3. Nanjing, China, Dec. 2015, pp. 1–3.
[19] R. R. Ramirez and F. De Flaviis, "A mutual coupling study of linear and circular polarized microstrip antennas for diversity wireless systems," *IEEE Trans. Antennas Propag.*, vol. 51, no. 2, pp. 238–248, Feb. 2003.
[20] K. C. Gupta, R. Garg, and I. J. Bahl, *Microstrip Lines and Slotlines*. Dedham, MA, USA: Artech House, 1979.
[21] R. E. Collin, *Foundations for Microwave Engineering*, 2nd ed. New York, NY, USA: Wiley, 1992.

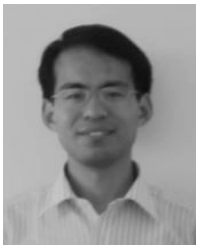

Guohua Zhai (M'15) was born in Shandong, China, in 1981. He received the B.Eng. degree in electric engineering from Qufu Normal University, Jining, China, in 2003, the M.Eng. degree in radio engineering from the Nanjing Institute of Electronic Technology, Nanjing, China, in 2006, and the Ph.D. degree in radio engineering from Southeast University, Nanjing, in 2009.

Since 2009, he has been with the Faculty of East China Normal University, Shanghai, China, as a Lecturer and later as an Associate Professor. Since 2013, he has been with the Institute for Infocomm Research, Singapore. His current research interests include microwave and millimeter-wave devices, and MIMO antenna system.

Zhi Ning Chen (M'99–SM'05–F'07) received the B.Eng., M.Eng., and Ph.D. degrees from the Institute of Communications Engineering (ICE), Nanjing, China, all in electrical engineering, and the Ph.D. degree from the University of Tsukuba, Tsukuba, Japan.

From 1988 to 1995, he was with ICE as a Lecturer and later as an Associate Professor, and Southeast University, Nanjing, as a Post-Doctoral Fellow and later as an Associate Professor. From 1995 to 1997, he was with the City University of Hong Kong, Hong Kong, as a Research Assistant and later as a Research Fellow. In 2004, he was with the IBM T. J. Watson Research Center, New York, NY, USA, as an Academic Visitor. From 1999 to 2012, he was with the Institute for Infocomm Research (I2R) as a Member of Technical Staff (MTS), a Senior MTS, the Principal MTS, a Senior Scientist, a Lead Scientist, and the Principal Scientist, and the Head of the RF and Optical Department. Since 2012, he has been with the Department of Electrical and Computer Engineering, National University of Singapore, as a Full Professor. He is currently an Advisor and the Principle Scientist with I2R. He holds Visiting/Adjunct/Guest Professor positions with Southeast University, Nanjing, Nanjing University, Nanjing, Shanghai Jiaotong University, Shanghai, Tsinghua University, Beijing, China, Tongji University, Shanghai, the University of Science and Technology of China, Hefei, China, Fudan University, Shanghai, as a Outstanding Overseas Professor, Dalian Maritime University, Dalian, China, Chiba University, Chiba, Japan, National Taiwan University of Science and Technology, Taipei, Taiwan, Shanghai University, Shanghai, as a Ziqiang Professor, and the City University of Hong Kong, Hong Kong. In 2013, he was a Senior DIGITEO Guest Scientist with the Laboratoire des Signauxet Systèmes, Centre national de la recherche scientifique, Supélec, University of Paris-Sud, Gif-sur-Yvette, France. In 2001 and 2004, he visited the University of Tsukuba under a Japan Society for the Promotion of Science (JSPS) Fellowship Program (senior level). He has authored 480 technical papers. He has authored and edited *Broadband Planar Antennas* (Wiley, 2005), *UWB Wireless Communication* (Wiley, 2006), *Antennas for Portable Devices* (Wiley, 2007), and *Antennas for Base Stations in Wireless Communications* (McGraw-Hill, 2009). He also contributed to *UWB Antennas and Propagation for Communications, Radar, and Imaging* (Wiley, 2006), *Antenna Engineering Handbook* (McGraw-Hill, 2007), and *Microstrip and Printed Antennas* (Wiley, 2010). He holds 30 granted and filed patents with 31 licensed deals with industry. His current research interests include electromagnetic engineering, antennas for microwaves, millimeter wave, submillimeter wave, and terahertz communication, radar, imaging and sensing systems.

Dr. Chen was a recipient of the International Symposium on Antennas and Propagation Best Paper Award in 2010, the CST University Publication Award in 2008, the IEEE Antennas and Propagation Society Honorable Mention Student Paper Contest in 2008, the Institution of Engineers Singapore Prestigious Engineering Achievement Awards 2006, 2013, and 2014, Singapore Manufacturing Federation Award 2014, the I2R Quarterly Best Paper Award 2004, and the IEEE iWAT 2005 Best Poster Award. He was also the recipient of the JSPS Fellowship to conduct his research at the University of Tsukuba in 1997. He has been the Founding General Chair of the International Workshop on Antenna Technology, the International Symposium on InfoComm and Media Technology in bio-medical and healthcare applications (IS 3T-in-3A), the International Microwave Forum, and the Asia–Pacific Conference on Antennas and Propagation. He is an Associate Editor of the IEEE TRANSACTIONS ON ANTENNAS AND PROPAGATION. He served the IEEE Antennas and Propagation Society as a Distinguished Lecturer from 2009 to 2011.

Xianming Qing (M'90–SM'15) received the B.Eng. degree in radio physics from the University of Electronic Science and Technology of China (UESTC), Chengdu, China, in 1985, and the Ph.D. degree in electrical engineering from Chiba University, Chiba, Japan, in 2010.

From 1987 to 1996, he was with UESTC involved with teaching and research and appointed as a Lecturer in 1990 and as an Associate Professor in 1995. He joined the National University of Singapore, Singapore, in 1997, as a Research Scientist. Since 1998, he has been with the Institute for Infocomm Research (I2R), Singapore. He is currently a Senior Scientist and the Head of the Antenna System Laboratory. He has authored or co-authored over 190 technical papers published in international journals or presented at international conferences, and five book chapters. He holds ten granted and filed patents. His current research interests include antenna design and characterization for wireless applications, small and broadband antennas/arrays for wireless systems, such as ultra-wideband, radio frequency identification, medical imaging, and microwave, millimeter wave, submillimeter wave, and terahertz imaging systems.

Dr. Qing has been a member of the IEEE Antennas and Propagation Society since 1990. He has been serving as a member of the RFID Technical Committee (TC-24) of the IEEE MTT-S since 2009. He was a recipient of The Institution of Engineers Singapore prestigious Engineering Achievement Award in 2006, 2013, and 2014. He was the recipient of six Advancement of Science and Technology Awards, China, from 1987 to 1997. He was also a recipient of the Singapore Manufacturing Federation Award in 2014 and the ISAP Best Paper Award in 2010. He severed as the Organizer and the Chair for special sessions on RFID antennas at the IEEE Antenna and Propagation Symposium in 2007 and 2008. He is serving as an Associate Editor for the *International Journal of Microwave and Wireless Technologies* (Cambridge Univ. Press/EuMA), the *International Journal of Microwave Science and Technology*, and the *International Journal of Antennas and Propagation* (Hindawi Publishing Corporation). He also served as a Guest Editor of the "Special Issue on Antennas for Emerging Radio Frequency Identification Applications" of the *International Journal on Wireless and Optical Communications*. He has served as a TPC member and the Session Chair for a number of conferences, and a regular Reviewer of the IEEE TRANSACTIONS ON ANTENNAS AND PROPAGATION, the IEEE TRANSACTIONS ON MICROWAVE THEORY AND TECHNIQUES, IEEE ANTENNAS AND WIRELESS PROPAGATION LETTERS, IEEE MICROWAVE AND WIRELESS COMPONENTS LETTERS, IET-MAP, and *Electronic Letters*.